# Phase estimation in lossy optical interferometry without a reference beam

Jun Tang, 1,\* Dong-Qing Wang, 1,\* Wei Zhong, 1,† Lan Zhou, 2 and Yu-Bo Sheng 3

1 Institute of Quantum Information and Technology,
Nanjing University of Posts and Telecommunications, Nanjing 210003, China
2 School of Science, Nanjing University of Posts and Telecommunications, Nanjing 210003, China
3 College of Electronic and Optical Engineering, Nanjing University
of Posts and Telecommunications, Nanjing 210003, China China

We investigate phase estimation in a lossy interferometer using entangled coherent states, with particular focus on a scenario where no reference beam is employed. By calculating the quantum Fisher information, we reveal two key results: (1) the metrological equivalence between scenarios with and without a reference beam, established under ideal lossless conditions for the two-phase-shifting configuration, breaks down in the presence of photon loss, and (2) the pronounced inferior performance of entangled coherent states relative to NOON states, observed in the presence of a reference beam, disappears in its absence.

# I. INTRODUCTION

Optical interferometers are among the most precise measurement instruments and have been widely employed in diverse fields, such as gravitational wave detection [1, 2], quantum imaging [3, 4], quantum ranging [5] and quantum lithography [6]. The ultimate sensitivity for estimating an unknown phase in an interferometer is typically determined by the state of input light. When classical light is used, the sensitivity is bounded by the shot noise limit  $1/\sqrt{N}$ , where N is the average photon number [7–9]. In contrast, non-classical states of light can surpass this limit. Among them, NOON states are particularly renowned for their ability to achieve Heisenberglimited sensitivity, which scales as 1/N [7–9]. More recently, entangled coherent states (ECSs) have emerged as promising candidates for phase estimation as they not only surpass the Heisenberg limit for small N but also exhibit greater robustness to photon loss compared to NOON states [10-17].

To fully leverage the advantages of non-classical light, an effective and sensitive measurement is required [18– In practical implementations, photon-numberresolving detectors constitute a crucial class of measurement schemes, such as parity and photon count [22–31]. These detectors are experimentally favorable, as they can be implemented without the need for a shared reference beam. However, previous studies on phase estimation with ECSs have been conducted under assumption that a common reference beam is already established [10-14, 17]. As a result, the findings reported in these works are generally not applicable to measurement schemes involving photon-number-resolving detectors. This naturally raises the question: how do ECSs perform in phase estimation when the reference beam is absent? More specifically, what is the ultimate phase sensitivity achievable for ECSs when using photon-number resolving detectors?

In this manuscript, we address this issue by reexamining the metrological performance of ECSs in a lossy interferometer. Using the quantum Fisher information (QFI) framework [18–21], we evaluate the ultimate sensitivity for both scenarios with and without a reference beam. Although it is commonly acknowledged that these two scenarios yield equivalent sensitivities under ideal lossless conditions for the two-phase-shifting configuration [15, 32], our results show that significant differences arise in the presence of photon loss. Specifically, not only does the equivalence break down, but also the disadvantage of ECSs relative to NOON states observed in the presence of reference beam also disappears when the reference beam is omitted.

This paper is organized as follows. In Sec. II, we introduce the two-mode optical interferometer and review the fundamentals of quantum estimation theory. Sec. III provides a comprehensive comparison of phase sensitivities for ECSs with and without a reference beam. Finally, we conclude in Sec. IV.

# II. PHASE ESTIMATION WITH A TWO-MODE OPTICAL INTERFEROMETER

A two-mode optical interferometer enables precise measurement of the phase difference between the two paths (see Fig. 1). A typical interferometer comprises two balanced beam splitters (BSs)  $B_i$  (i=1,2) and a phase shifter  $U_{\phi}$  with an unknown phase parameter  $\phi$  [33]. As photons propagate between the BSs, the phase of interest is accumulated. The overall interferometric evolution can be described by the composite operator  $K = B_2 U_{\phi} B_1$ . If  $\rho_{\rm in}$  denotes the state entering the interferometer, then the output state is given by  $\rho_{\rm out} = K \rho_{\rm in} K^{\dagger}$ . Measurements performed at the output ports provide information to estimate the unknown phase parameter.

For convenience, we refer to the probe state as the state prior to the phase-shifting operation, i.e.,  $\rho = B_1 \rho_{\rm in} B_1^{\dagger}$ . Under the action of the phase shifter  $U_{\phi}$ , the state evolves

<sup>\*</sup> These authors contributed equally to this work

<sup>†</sup> zhongwei1118@gmail.com

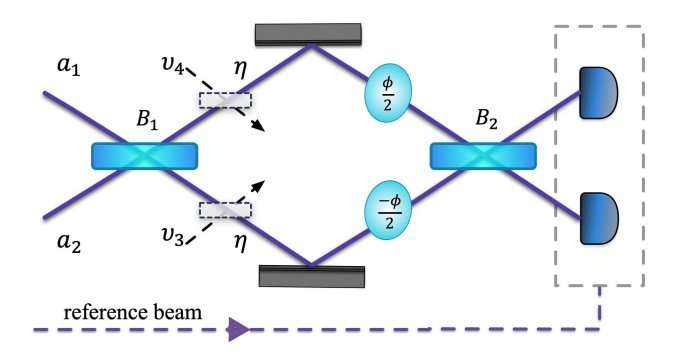


Figure 1. Schematic of a two-mode lossy optical interferometer.

into the phase-encoded state  $\rho_{\phi} = U_{\phi} \rho U_{\phi}^{\dagger}$ . According to quantum estimation theory, the quantum Cramér-Rao theorem sets a fundamental lower bound on the phase uncertainty  $\delta \hat{\phi}$  for any locally unbiased estimator  $\hat{\phi}$  [18, 34, 35]:

$$\delta \hat{\phi} \geqslant (mF)^{-1/2}, \tag{1}$$

where m is the number of repetitions of an experiment, and F is the QFI defined as  $F = \text{Tr} \left( \rho_{\phi} L^2 \right)$ . Here, L is the symmetric logarithmic derivative operator implicitly defined by  $\partial \rho_{\phi}/\partial \phi = \left( \rho_{\phi} L + L \rho_{\phi} \right)/2$ . This bound is asymptotically achievable and serves as a benchmark for assessing the performance of phase estimation protocols. In interferometric phase estimation, the QFI depends solely on the phase-encoded state  $\rho_{\phi}$ , regardless of the second BS  $B_2$  due to the  $\phi$ -independent unitary invariance of the QFI [36].

We consider two commonly used forms of phase-shifting unitary operators. The first is the two-arm phase shift

$$U_{\phi}^{T} = \exp\left[-i\phi\left(a_{1}^{\dagger}a_{1} - a_{2}^{\dagger}a_{2}\right)/2\right],\tag{2}$$

which in introduce a difference phase shift by applying phase shifts of  $\phi/2$  and  $-\phi/2$  to the two interferometer paths, respectively. Here,  $a_i$  and  $a_i^\dagger$  denote the annihilation and creation operators for the ith mode (i=1,2), respectively. The second is the single-arm phase shift  $U_\phi^S=e^{-i\phi a_1^\dagger a_1},$  which applies the full phase shift  $\phi$  to a single path. Notably, these two phase-shifting operators are metrologically equivalent in the absence of reference beam [15, 32]. This equivalence stems from the fact that  $U_\phi^S$  differs from  $U_\phi^T$  only up to a sum phase shift  $U_\phi^\&=\exp[-i\phi(a_1^\dagger a_1+a_2^\dagger a_2)/2],$  which is experimentally immeasurable without introducing an external phase reference

More precisely, in reference-free scenarios, the probe state must be phase-averaged as [32, 37]

$$\varrho = \int_{-\pi}^{\pi} \frac{d\theta}{2\pi} U_{\theta}^{a_1} U_{\theta}^{a_2} \rho U_{\theta}^{a_1 \dagger} U_{\theta}^{a_2 \dagger}, \tag{3}$$

with  $U_{\theta}^{x}=\exp(-i\theta x^{\dagger}x)$ . The resulting phase-averaged state is a statistical ensemble of states with fixed photon numbers, resulting in the loss of coherence between different photon-number subspaces. Consequently, such states are insensitive to  $U_{\phi}^{\mathcal{S}}$ , rendering  $U_{\phi}^{S}$  and  $U_{\phi}^{T}$  operationally indistinguishable in phase estimation. In other words, for given a probe state, the ultimate phase sensitivity is independent of the specific form of the phase-shifting operation in the absence of a reference beam. However, once a external reference beam is established, the sum phase becomes physically meaningful, and the two configurations  $U_{\phi}^{S}$  and  $U_{\phi}^{T}$  become distinguishable, leading to potentially different metrological performances.

In this work, we focus on the  $U_\phi^T$  configuration for the following reasons: (1) In the ideal lossless case, the QFI under  $U_\phi^T$  is identical irrespective of the presence or absence of a reference beam. However, whether this equivalence persists under photon loss remains an open question, which is one of issues we aim to address. (2) The  $U_\phi^S$  configuration has been extensively studied in previous studies [11–14, 16], and the methodology developed here for  $U_\phi^T$  can be straightforwardly adapted to analyze  $U_\phi^S$  as well.

# III. PHASE SENSITIVITY OF LOSSY INTERFEROMETRY WITH ECSS

In this section, we investigate the phase sensitivity of a lossy interferometer using ECSs as the probe state. Photon loss is modeled by inserting a virtual BS with transmittance  $\eta$  into each interferometer path, denoted by the operator  $V_{\eta}$  [12, 38, 39]. For simplicity, we assume equal photon loss in both interferometer paths. ECSs can be generated by mixing coherent and coherent superposition states of light on a BS [10], or alternatively generated by mixing coherent and squeezed vacuum states of light on a BS [40]. The resulting ECS is given by

$$|ECS\rangle = \mathcal{N}(|\alpha\rangle|0\rangle + |0\rangle|\alpha\rangle),$$
 (4)

with normalization coefficient  $\mathcal{N}=1/\sqrt{2(1+e^{-|\alpha|^2})}$ . This state can be expanded as a superposition of NOON states

$$|ECS\rangle = \sqrt{2}\mathcal{N}\sum_{n=0}^{\infty} |c_n|^2 |n::0\rangle,$$
 (5)

where  $c_n = e^{-|\alpha|^2/2} \alpha^n / \sqrt{n!}$ , and  $|n::0\rangle \equiv (|n\rangle|0\rangle + |0\rangle|n\rangle) / \sqrt{2}$  denotes a NOON state with fixed photon number n. The average photon number of the ECS is  $\overline{N} = 2\mathcal{N}^2 |\alpha|^2$ . In the limit of large  $|\alpha|$ , this approaches  $\overline{N} \sim |\alpha|^2$  since  $\mathcal{N} \sim 1/\sqrt{2}$ . In what follows, we compute the QFI for ECS-based phase estimation within two distinct scenarios: with and without a reference beam.

# A. Phase sensitivity without a reference beam

We first consider the scenario in which no reference beam is available. In this case, the phase-averaging operation defined in Eq. (3) must be applied. As a result, the ECS probe state given in Eq. (4) becomes a mixed state, which can be expressed as a direct sum of weighted NOON states [15, 36]

$$\varrho_{\text{ECS}} = 2\mathcal{N}^2 \bigoplus_{n=0}^{\infty} |c_n|^2 |n :: 0\rangle \langle n :: 0|.$$
 (6)

According to the additivity property of the QFI, the QFI for this phase-averaged ECS can be directly calculated as

$$F_{\varrho} = 2\mathcal{N}^2 \sum_{n=0}^{\infty} |c_n|^2 F_{\text{noon}}, \tag{7}$$

where  $F_{\text{noon}} = n^2 \eta^n$  is the QFI for small NOON states used as probe states in a lossy interferometer [13, 31]. Equation (7) can be expressed in the compact form

$$F_{\varrho} = 2\mathcal{N}^2 e^{-|\alpha|^2 (1-\eta)} \left( |\alpha|^4 \eta^2 + |\alpha|^2 \eta \right).$$
 (8)

In this expression, the first term inside the parentheses represents the Heisenberg-scaling contribution, while the second term corresponds to shot-noise scaling. This result is valid for both the single-phase and two-phase configurations  $(U_\phi^S \text{ and } U_\phi^T),$  as justified in preceding section. In the ideal lossless case  $(\eta=1)$ , the QFI simplifies to [15]

$$F_{\rho} = 2\mathcal{N}^2 \left( |\alpha|^4 + |\alpha|^2 \right). \tag{9}$$

Expressing in terms of mean photon number, we have  $F_{\varrho} \geq \overline{N}^2 + \overline{N}$ , thereby surpassing the conventional Heisenberg limit. This result demonstrates that ECSs offer superior phase sensitivity compared to NOON states with the same average photon number.

#### B. Phase sensitivity with a reference beam

For comparison, we now consider the scenario in which a common reference beam is available, and the probe state is the pure ECS defined in Eq. (4). In this case, the phase-shifting operation is implemented using the operator  $U_{\phi}^{T}$ . Unlike the reference-free scenario, calculating the QFI in the presence of a reference beam is more intricate. Below, we summarize the key steps in the calculation, while full derivations are provided in Appendix.

Owing to the commutation relationship between photon loss and phase shifting [38, 39], the order of these operations can be interchanged without affecting the final measurement results. Thus, we assume that the ECS in Eq. (4) first undergoes photon loss, followed by the

phase accumulation process. Under such loss, the ECS evolves into a mixed state as

$$\sigma_{\text{ECS}} = \text{Tr}_{34} \Big[ V_{13} V_{24} \left( |\text{ECS}\rangle_{12} \langle \text{ECS}| \otimes |00\rangle_{34} \langle 00| \right) V_{24}^{\dagger} V_{13}^{\dagger} \Big]$$

$$= \mathcal{N}^{2} \Big( |\alpha\sqrt{\eta}, 0\rangle \langle \alpha\sqrt{\eta}, 0| + |0, \alpha\sqrt{\eta}\rangle \langle 0, \alpha\sqrt{\eta}| + e^{-(1-\eta)|\alpha|^{2}} |\alpha\sqrt{\eta}, 0\rangle \langle 0, \alpha\sqrt{\eta}| + e^{-(1-\eta)|\alpha|^{2}} |0, \alpha\sqrt{\eta}\rangle \langle 0, \alpha\sqrt{\eta}| + e^{-(1-\eta)|\alpha|^{2}} |0, \alpha\sqrt{\eta}\rangle \langle \alpha\sqrt{\eta}, 0| \Big),$$

$$(10)$$

where  $|0\rangle_k$  (k=3,4) denote the vacuum states of the environmental modes corresponding to paths 1 and 2, respectively. Here the virtual beam splitters are defined as  $V_{13}$  and  $V_{24}$  define  $V_{13} = \exp[\arccos\sqrt{\eta}(a_1^{\dagger}v_3 - a_1v_3^{\dagger})]$ , and  $V_{24}$  is defined analogously by substituting modes 1 and 3 with modes 2 and 4. Let  $|\Psi_1\rangle = |\alpha\sqrt{\eta},0\rangle$  and  $|\Psi_2\rangle = |0,\alpha\sqrt{\eta}\rangle$ . These states are non-orthogonal, with overlap  $p \equiv \langle \Psi_1 | \Psi_2 \rangle = e^{-\eta |\alpha|^2}$ . Employing the Gram-Schmidt orthogonalization and performing spectral decomposition [14, 16], the state  $\sigma_{\rm ECS}$  can be diagonalized as

$$\sigma_{\rm ECS} = \gamma_{+}|\gamma_{+}\rangle\langle\gamma_{+}| + \gamma_{-}|\gamma_{-}\rangle\langle\gamma_{-}|,$$
 (11)

where the eigenstates take the form

$$|\gamma_{\pm}\rangle = \mathcal{C}_{\pm} |\Psi_1\rangle + \mathcal{D}_{\mp} |\Psi_2\rangle,$$
 (12)

and the corresponding eigenvalues are given by

$$\gamma_{\pm} = \frac{1}{2} \left( 1 \pm \sqrt{1 - \det \sigma_{\text{ECS}}} \right). \tag{13}$$

In Eq. (12), the expansion coefficients are defined as

$$C_{\pm} = \pm \zeta_{\pm} - p \mathcal{D}_{\mp}, \ \mathcal{D}_{\mp} = \frac{\zeta_{\mp}}{\sqrt{1 - p^2}},$$
 (14)

with  $\zeta_{\pm} = \sqrt{\frac{\sqrt{1-4 \det \sigma_{\text{ECS}}} \pm \langle \sigma_3 \rangle}{2\sqrt{1-4 \det \sigma_{\text{ECS}}}}}$ ,  $\det \sigma_{\text{ECS}} = \mathcal{N}^4 (1-p^2) (1-p^2)$ ,  $\langle \sigma_3 \rangle = 1 - 2\mathcal{N}^2 (1-p^2)$  and  $p_{\perp} = e^{-(1-\eta)|\alpha|^2}$ .

The QFI for the mixed state  $\sigma_{\rm ECS}$  is then obtained by

$$F_{\sigma} = 4\left(\gamma_{+}\Delta^{2}G_{+} + \gamma_{-}\Delta^{2}G_{-} - 4\gamma_{+}\gamma_{-}|G_{+-}|^{2}\right), (15)$$

where

$$\Delta^{2}G_{\pm} = \langle \gamma_{\pm} | G^{2} | \gamma_{\pm} \rangle - \langle \gamma_{\pm} | G | \gamma_{\pm} \rangle^{2}, \qquad (16)$$

$$G_{+-} = \langle \gamma_{+} | G | \gamma_{-} \rangle, \qquad (17)$$

and  $G = (a_1^{\dagger} a_1 - a_2^{\dagger} a_2)/2$  is the generator of  $U_{\phi}^T$  defined in Eq. (2). To compute  $\Delta^2 G_{\pm}$  and  $G_{+-}$ , we use the following expectation values

$$\langle \Psi_1 | G | \Psi_1 \rangle = \frac{1}{2} |\alpha|^2 \eta, \quad \langle \Psi_2 | G | \Psi_2 \rangle = -\frac{1}{2} |\alpha|^2 \eta, (18)$$

$$\langle \Psi_i | G^2 | \Psi_i \rangle = \frac{1}{4} (|\alpha|^2 \eta + |\alpha|^4 \eta^2), \text{ for } i = 1, 2, \quad (19)$$

$$\langle \Psi_1 | G | \Psi_2 \rangle = \langle \Psi_1 | G^2 | \Psi_2 \rangle = 0.$$
 (20)

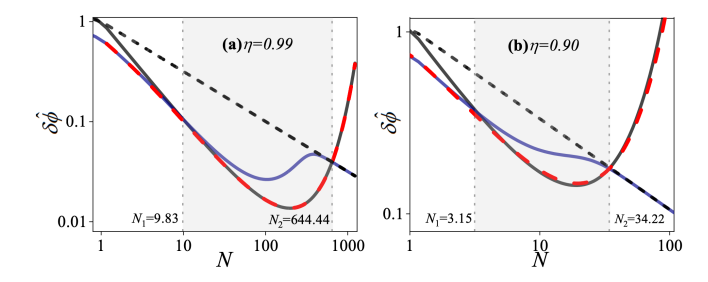


Figure 2. Log-log plot of phase sensitivity as a function of the mean photon number N (with  $\overline{N}=N$  for ECSs) for (a)  $\eta=0.99$  and (b)  $\eta=0.9$ . The blue solid line and red dashed line represent ECSs with and without a reference beam, respectively. The black solid line corresponds to the NOON states, and the gray dashed line marks the shot-noise limit  $1/\sqrt{\eta N}$  as a benchmark.

Substituting these into Eq. (15) yields the full expression for  $F_{\sigma}$ . Although this expression is algebraically cumbersome, it simplifies, in the limit  $p \to 0$  (i.e.,  $\eta |\alpha|^2 \gg 1$ ), to

$$F_{\sigma} = 2\mathcal{N}^2 \left( e^{-2|\alpha|^2(1-\eta)} |\alpha|^4 \eta^2 + |\alpha|^2 \eta \right).$$
 (21)

In the ideal lossless case  $(\eta=1)$ , this expression reduces to Eq. (9), i.e.,  $F_\varrho=F_\sigma$ , thereby confirming that, for the two-phase-shifting operation  $U_\phi^T$ , the metrological performance remains invariant regardless of the presence or absence of a reference beam. This result is consistent with the commonly acknowledged conclusion reported in [15, 32], namely that the phase shifter  $U_\phi^T$  exhibits metrological equivalence between scenarios with and without a reference beam for phase estimation protocols employing pure probe states. However, as we demonstrate below, in the presence of photon loss, ECSs with and without a reference beam exhibit distinct metrological behavior, indicating that this equivalence does not extend to lossy conditions.

# C. Further comparison

To thoroughly assess metrological performance under photon loss, we compare three quantum strategies: (i) ECSs without a reference beam, (ii) ECSs with a reference beam, and (iii) NOON states, whose QFI is given by  $F_{\rm NOON} = \eta^N N^2$  [13, 31]. For a fair comparison, we set the same mean photon number  $\overline{N} = N$  for both ECSs and NOON states.

Let us first compare the strategies of NOON states and ECSs with a reference beam. As shown in Fig. (2), the two critical crossing points  $N_1$  and  $N_2$  exist, defined by the condition  $F_{\text{NOON}} = F_{\sigma}$ . Although their analytical expressions are cumbersome, these crossing points demarcate distinct performance regimes. In the regime  $N < N_1$ , ECSs with a reference beam outperforms NOON

states. However, in the intermediate range  $N_1 < N < N_2$ , this trend reverses with NOON states exhibiting superior performance against ECSs. As N increases further, the QFI of NOON states diverges, whereas the QFI of ECSs with a reference beam asymptotically approaches the shot-noise limit  $(\delta \phi \sim 1/\sqrt{\eta N})$ . This phenomenon illustrates that although the use of a reference beam enables ECSs to achieve superior sensitivity compared to NOON states at low N, this advantage diminishes at intermediate N. A similar trend has been reported for the single-phase configuration  $U_{\phi}^{S}$  [13]. Interestingly, ECSs without a reference beam combines the advantages of both strategies: for  $N < N_1$ , they perform similarly to ECSs with a reference beam, while for  $N > N_1$ , they resemble NOON states. Consequently, although phase sensitivity deteriorates with increasing loss, omitting the reference beam can be advantageous in ECS-based phase estimation, offering improved performance across a border range of photon numbers.

These behaviors are quantitatively supported by Eqs. (8) and (21). In the low intensity regime, where  $|\alpha|^2(1-\eta) \ll 1$ , we have  $e^{-2|\alpha|^2(1-\eta)} \sim 1$ , which leads to

$$F_{\varrho} = F_{\sigma} \approx 2\mathcal{N}^2 \left( |\alpha|^4 \eta^2 + |\alpha|^2 \eta \right).$$
 (22)

This explains why, in Fig. (2), the QFIs of both ECS strategies nearly coincide in the low-photon-number regime. In the high intensity regime  $\overline{N} \sim |\alpha|^2 \gg 1$ , however, the behavior diverges. For ECSs with a reference beam, the first term in Eq. (21) (which corresponds to the Heisenberg-limit scaling) vanishes due to  $e^{-2|\alpha|^2(1-\eta)} \to 0$ . This leaves only the second term, which scales as shot noise limit:  $F_{\sigma} \sim \eta \overline{N}$ . By contrast, for ECSs without a reference beam, the behavior resembles that of NOON states in this regime. Recalling that  $\overline{N} = |\alpha|^2$ , the QFI from Eq. (8) becomes

$$F_{\varrho} \ = \ e^{\left(\overline{N}+2\right)(\eta-1)}\overline{N}^2 + e^{\overline{N}(\eta-1)}\overline{N}\eta \approx e^{\overline{N}(\eta-1)}\overline{N}^2 (23)$$

This scaling is consistent with that of NOON states, for which

$$F_{\text{NOON}} = \eta^N N^2 \approx e^{N(\eta - 1)} N^2, \tag{24}$$

where we have used the approximation  $\ln \eta \sim \eta - 1$  in the limit  $\eta \rightarrow 1$ .

#### IV. CONCLUSION

In this work, we systematically analyzed the phase estimation performance of a lossy optical interferometer using ECSs as probe states, considering scenarios both with and without a reference beam. Using the QFI as a metric, we demonstrated that photon loss breaks the metrological equivalence between these two scenarios in the two-phase-shifting configuration. Furthermore, we

showed that omitting the reference beam may be beneficial for improving the sensitivity of ECS-based interferometric phase estimation. These findings provide valuable insights into lossy interferometry and the development of practical quantum metrology schemes.

#### ACKNOWLEDGMENTS

This work was supported by the NSFC through Grant No. 12005106 and the Postgraduate Research and Practice Innovation Program of Jiangsu Province (Grant No. JSCX23-0260).

#### APPENDIX: DETAILED DERIVATIONS

In this appendix, we present the detailed derivations of Eqs. (10), (11) and (15) from the main text.

# A. Derivation of Eq. (10)

For a lossy interferometer, photon losses are modeled by inserting two virtual BSs  $V_{13}$  and  $V_{24}$  into each interferometer path. The BS  $V_{13}$  is defined as

$$V_{13} = \exp\left[\arccos\sqrt{\eta}\left(a_1^{\dagger}v_3 - a_1v_3^{\dagger}\right)\right], \quad (A1)$$

where the subscripts 1 and 3 represent the interferometer path 1 and its corresponding environment mode 3, which is initially in the vacuum state. Similarly,  $V_{24}$  acts on modes 2 and 4 in the same form, with 1 and 3 replaced by 2 and 4. Both BSs have equal transmittance  $\eta$ . The input and output relations for  $V_{13}$  are

$$V_{13}^{\dagger} a_1 V_{13} = \sqrt{\eta} a_1 + \sqrt{1 - \eta} v_3,$$
 (A2)

$$V_{13}^{\dagger} v_3 V_{13} = -\sqrt{1 - \eta} a_1 + \sqrt{\eta} v_3. \tag{A3}$$

Applying these, one obtains

$$V_{13}|\alpha\rangle_1|0\rangle_3 = |\alpha\sqrt{\eta}\rangle_1|-\sqrt{1-\eta}\alpha\rangle_3.$$
 (A4)

and similarly

$$V_{24}|\alpha\rangle_2|0\rangle_4 = |\alpha\sqrt{\eta}\rangle_2|-\sqrt{1-\eta}\alpha\rangle_4.$$
 (A5)

The total state after loss becomes

$$V_{1,3}V_{2,4} | ECS \rangle_{12} |00\rangle_{3,4}$$

$$= V_{1,3}V_{2,4}\mathcal{N}(|\alpha\rangle_{1}|0\rangle_{2} + |0\rangle_{1}|\alpha\rangle_{2})|00\rangle_{3,4}$$

$$= \mathcal{N}\left(|\alpha\sqrt{\eta}\rangle_{1}|0\rangle_{2}|-\sqrt{1-\eta}\alpha\rangle_{3}|0\rangle_{4} + |0\rangle_{1}|\alpha\sqrt{\eta}\rangle_{2}|0\rangle_{3}|-\sqrt{1-\eta}\alpha\rangle_{4}\right). \quad (A6)$$

Tracing over the environment modes 3 and 4 yields the reduced density matrix for mode 1 and 2

$$\sigma_{\text{ECS}} = \text{Tr}_{34} \Big[ V_{13} V_{24} \left( |\text{ECS}\rangle_{12} \langle \text{ECS}| \otimes |00\rangle_{34} \langle 00| \right) V_{24}^{\dagger} V_{13}^{\dagger} \Big]$$

$$= \mathcal{N}^{2} \Big( |\alpha\sqrt{\eta}, 0\rangle_{12} \langle \alpha\sqrt{\eta}, 0| + |0, \alpha\sqrt{\eta}\rangle_{12} \langle 0, \alpha\sqrt{\eta}| + e^{-(1-\eta)|\alpha|^{2}} |\alpha\sqrt{\eta}, 0\rangle_{12} \langle 0, \alpha\sqrt{\eta}| + e^{-(1-\eta)|\alpha|^{2}} |0, \alpha\sqrt{\eta}\rangle_{12} \langle 0, \alpha\sqrt{\eta}, 0| \Big), \tag{A7}$$

where we have used the overlap of coherent states

$$|\langle \alpha | \beta \rangle|^2 = e^{-|\alpha - \beta|^2}.$$
 (A8)

Defining the non-orthogonal basis

$$|\Psi_1\rangle \equiv |\alpha\sqrt{\eta}, 0\rangle_{12}, |\Psi_2\rangle \equiv |0, \alpha\sqrt{\eta}\rangle_{12},$$
 (A9)

the density matrix  $\sigma_{\rm ECS}$  can be written as

$$\sigma_{\text{ECS}} = \mathcal{N}^2 \begin{pmatrix} 1 & e^{-(1-\eta)|\alpha|^2} \\ e^{-(1-\eta)|\alpha|^2} & 1 \end{pmatrix}. \quad (A10)$$

#### B. Derivation of Eq. (11)

Since the basis  $\{|\Psi_1\rangle, |\Psi_2\rangle\}$  form a non-orthogonal basis with overlap

$$p \equiv \langle \Psi_1 | \Psi_2 \rangle = e^{-\eta |\alpha|^2}, \tag{B1}$$

we use the Gram-Schmidt procedure [41] to construct an orthogonal basis

$$|\Phi_1\rangle = |\Psi_1\rangle, \ |\Phi_2\rangle = \frac{1}{\sqrt{1-p^2}}(|\Psi_2\rangle - p |\Psi_1\rangle).$$
 (B2)

In this basis, the density matrix  $\sigma_{ECS}$  becomes

$$\sigma_{\rm ECS} = \mathcal{N}^2 \begin{pmatrix} 1 + 2pp_{\perp} + p^2 & (p + p_{\perp})\sqrt{1 - p^2} \\ (p + p_{\perp})\sqrt{1 - p^2} & (1 - p^2) p_{\perp} \end{pmatrix}, \text{ (B3)}$$

with  $p_{\perp} \equiv e^{-(1-\eta)|\alpha|^2}$ . Diagonalizing  $\sigma_{\rm ECS}$ , the spectral decomposition reads

$$\sigma_{\rm ECS} = \gamma_{+}|\gamma_{+}\rangle\langle\gamma_{+}| + \gamma_{-}|\gamma_{-}\rangle\langle\gamma_{-}|,$$
 (B4)

with eigenvalues

$$\gamma_{\pm} = \frac{1}{2} \left( 1 \pm \sqrt{1 - \det \sigma_{\text{ECS}}} \right).$$
(B5)

The corresponding eigenstates are

$$|\gamma_{\pm}\rangle = (\pm \zeta_{\pm} e^{i\vartheta}, \zeta_{\mp})^{\mathrm{T}},$$
 (B6)

where  $\zeta_{\pm}$  are defined in the main text. When transformed into the original non-orthogonal basis  $\{|\Psi_1\rangle, |\Psi_2\rangle\}$ , these eigenstates can be expressed as

$$|\gamma_{\pm}\rangle = \mathcal{C}_{\pm} |\Psi_1\rangle + \mathcal{D}_{\mp} |\Psi_2\rangle,$$
 (B7)

with

$$C_{\pm} = \pm \zeta_{\pm} - p \mathcal{D}_{\mp}, \ \mathcal{D}_{\mp} = \frac{\zeta_{\mp}}{\sqrt{1 - p^2}}.$$
 (B8)

#### C. Derivation of Eq. (15)

Consider a general  $d\times d$  density matrix  $\rho$  with spectral decomposition

$$\rho = \sum_{i=1}^{d} p_i |\psi_i\rangle \langle \psi_i|. \tag{C1}$$

Assuming the unknown parameter  $\phi$  to be encoded via the unitary operator  $U_{\phi} = e^{-iG\phi}$ , where G is the generator, the resulting parameter-dependent state is

$$\rho_{\phi} = U_{\phi} \rho U_{\phi}^{\dagger} = \sum_{i} p_{i} |\psi_{i} (\phi)\rangle \langle \psi_{i} (\phi)|, \quad (C2)$$

where  $|\psi_i(\phi)\rangle = U_\phi |\psi_i\rangle$ . The QFI can be computed by [14, 42]

$$F = 4 \sum_{i=1}^{d} p_i \Delta^2 G_{ii} - \sum_{i \neq j} \frac{8p_i p_j}{p_i + p_j} |G_{ij}|^2, \quad (C3)$$

where

$$\Delta^2 G_{ii} = \langle \psi_i | G^2 | \psi_i \rangle - \langle \psi_i | G | \psi_i \rangle^2, \qquad (C4)$$

$$G_{ij} = \langle \psi_i | G | \psi_j \rangle. \tag{C5}$$

For the two-dimensional case of Eq. (B4), the QFI simplifies to

$$F = 4 \left( \lambda_{+} \Delta^{2} G_{+} + \lambda_{-} \Delta^{2} G_{-} - 4 \lambda_{+} \lambda_{-} |G_{+-}|^{2} \right), (C6)$$

where

$$\Delta^{2}G_{\pm} = \langle \lambda_{\pm} | G^{2} | \lambda_{\pm} \rangle - \langle \lambda_{\pm} | G | \lambda_{\pm} \rangle^{2}, \quad (C7)$$

$$G_{+-} = \langle \lambda_{+} | G | \lambda_{-} \rangle. \tag{C8}$$

- [1] M. Tse and et. al., Phys. Rev. Lett. **123**, 231107 (2019).
- [2] F. Acernese and M. e. Agathos (Virgo Collaboration), Phys. Rev. Lett. 123, 231108 (2019).
- [3] H. Defienne, W. P. Bowen, M. Chekhova, G. B. Lemos, D. Oron, S. Ramelow, N. Treps, and D. Faccio, Nature Photonics 18, 1024 (2024).
- [4] R.-B. Jin, Z.-Q. Zeng, C. You, and C. Yuan, Progress in Quantum Electronics 96, 100519 (2024).
- [5] G. Qian, X. Xu, S.-A. Zhu, C. Xu, F. Gao, V. V. Yakovlev, X. Liu, S.-Y. Zhu, and D.-W. Wang, Phys. Rev. Lett. 131, 033603 (2023).
- [6] M. D'Angelo, M. V. Chekhova, and Y. Shih, Phys. Rev. Lett. 87, 013602 (2001).
- [7] V. Giovannetti, S. Lloyd, and L. Maccone, Science **306**, 1330 (2004).
- [8] V. Giovannetti, S. Lloyd, and L. Maccone, Nat. Photon. 5, 222 (2011).
- [9] V. Giovannetti, S. Lloyd, and L. Maccone, Phys. Rev. Lett. 96, 010401 (2006).
- [10] A. Luis, Phys. Rev. A 64, 054102 (2001).
- [11] J. Joo, W. J. Munro, and T. P. Spiller, Phys. Rev. Lett. 107, 083601 (2011).
- [12] J. Joo, K. Park, H. Jeong, W. J. Munro, K. Nemoto, and T. P. Spiller, Phys. Rev. A 86, 043828 (2012).
- [13] Y. M. Zhang, X. W. Li, W. Yang, and G. R. Jin, Phys. Rev. A 88, 043832 (2013).
- [14] X.-X. Jing, J. Liu, W. Zhong, and X.-G. Wang, Communications in Theoretical Physics 61, 115 (2014).
- [15] W. Zhong, L. Zhou, C.-F. Zhang, and Y.-B. Sheng, Quantum Information Processing 22, 56 (2023).
- [16] J. Tang, Z.-H. Du, W. Zhong, L. Zhou, and Y.-B. Sheng, Chinese Physics B 34, 020303 (2025).
- [17] X. Yu, X. Zhao, L. Shen, Y. Shao, J. Liu, and X. Wang, Opt. Express 26, 16292 (2018).

- [18] S. L. Braunstein and C. M. Caves, Phys. Rev. Lett. 72, 3439 (1994).
- [19] S. L. Braunstein, C. M. Caves, and G. Milburn, Annals of Physics 247, 135 (1996).
- [20] M. A. T. T. E. O. G. A. PARIS, Int. J. Quantum Inform. **07**, 125 (2009).
- [21] W. Zhong, X. M. Lu, X. X. Jing, and X. G. Wang, J. Phys. A: Math. Theor. 47, 385304 (2014).
- [22] R. A. Campos, C. C. Gerry, and A. Benmoussa, Phys. Rev. A 68, 023810 (2003).
- [23] H. F. Hofmann, Phys. Rev. A 79, 033822 (2009).
- [24] W. N. Plick, P. M. Anisimov, J. P. Dowling, H. Lee, and G. S. Agarwal, New J. Phys. 12, 113025 (2010).
- [25] A. Chiruvelli and H. Lee, J. Mod. Opt. 58, 945 (2011).
- [26] K. P. Seshadreesan, P. M. Anisimov, H. Lee, and J. P. Dowling, New J. Phys. 13, 083026 (2011).
- [27] K. P. Seshadreesan, S. Kim, J. P. Dowling, and H. Lee, Phys. Rev. A 87, 043833 (2013).
- [28] L. Pezzé and A. Smerzi, Phys. Rev. Lett. 110, 163604 (2013).
- [29] W. Zhong, Y. Huang, X. Wang, and S. L. Zhu, Phys. Rev. A 95, 052304 (2017).
- [30] G. S. Thekkadath, M. E. Mycroft, B. A. Bell, C. G. Wade, A. Eckstein, D. S. Phillips, R. B. Patel, A. Buraczewski, A. E. Lita, T. Gerrits, S. W. Nam, M. Stobińska, A. I. Lvovsky, and I. A. Walmsley, npj Quantum Information 6, 89 (2020).
- [31] W. Zhong, L. Zhou, and Y.-B. Sheng, Phys. Rev. A 103, 042611 (2021).
- [32] M. Jarzyna and R. Demkowicz-Dobrzański, Phys. Rev. A 85, 011801(R) (2012).
- [33] B. Yurke, S. L. McCall, and J. R. Klauder, Phys. Rev. A 33, 4033 (1986).
- [34] C. W. Helstrom, Quantum Detection and Estimation Theory (Academic, New York, 1976).

- [35] A. S. Holevo, Probabilistic and Statistical Aspects of Quantum Theory (North-Holland, Amsterdam, 1982).
- [36] J. Liu, H. Yuan, X.-M. Lu, and X. Wang, J. Phys. A: Math. Theor. 53, 023001 (2019).
- [37] S. D. Bartlett, T. Rudolph, and R. W. Spekkens, Rev. Mod. Phys. 79, 555 (2007).
- [38] U. Dorner, R. Demkowicz-Dobrzanski, B. J. Smith, J. S. Lundeen, W. Wasilewski, K. Banaszek, and I. A. Walmsley, Phys. Rev. Lett. 102, 040403 (2009).
- [39] R. Demkowicz-Dobrzanski, U. Dorner, B. J. Smith, J. S. Lundeen, W. Wasilewski, K. Banaszek, and I. A. Walm-

- sley, Phys. Rev. A 80, 013825 (2009).
- [40] Y. Israel, L. Cohen, X.-B. Song, J. Joo, H. S. Eisenberg, and Y. Silberberg, Optica 6, 753 (2019).
- [41] M. A. Nielsen and I. L. Chuang, Quantum Computation and Quantum Information (Cambridge University Press, Cambridge, 2000).
- [42] W. Zhong, Z. Sun, J. Ma, X. Wang, and F. Nori, Phys. Rev. A 87, 022337 (2013).